

Ferromagnetic Kitaev interaction and the origin of large magnetic anisotropy in α -RuCl₃

J. A. Sears,¹ Li Ern Chern,² Subin Kim,² P. J. Bereciartua,¹ S. Francoual,¹ Yong Baek Kim,² and Young-June Kim²

¹*Deutsches Elektronen-Synchrotron (DESY), 22607 Hamburg, Germany*

²*Department of Physics, University of Toronto, 60 St. George St., Toronto, Ontario, M5S 1A7, Canada*

(Dated: October 30, 2019)

α -RuCl₃ is drawing much attention as a promising candidate Kitaev quantum spin liquid [1–8]. However, despite intensive research efforts, controversy remains about the form of the basic interactions governing the physics of this material. Even the sign of the Kitaev interaction (the bond-dependent anisotropic interaction responsible for Kitaev physics) is still under debate, with conflicting results from theoretical and experimental studies [5, 6, 9–15]. The significance of the symmetric off-diagonal exchange interaction (referred to as the Γ term) is another contentious question [16–18]. Here, we present resonant elastic x-ray scattering data that provides unambiguous experimental constraints to the two leading terms in the magnetic interaction Hamiltonian. We show that the Kitaev interaction (K) is ferromagnetic, and that the Γ term is antiferromagnetic and comparable in size to the Kitaev interaction. Our findings also provide a natural explanation for the large anisotropy of the magnetic susceptibility in α -RuCl₃ as arising from the large Γ term. We therefore provide a crucial foundation for understanding the interactions underpinning the exotic magnetic behaviours observed in α -RuCl₃.

The magnetic behaviour of the honeycomb material α -RuCl₃ has been the topic of much recent work, following the discovery in this material of an unusual continuum of magnetic excitations not well explained by spin-wave theory [3, 5, 6]. The structural environment and electronic state of the ruthenium atoms in α -RuCl₃ are such that the Kitaev magnetic interaction [19] is expected to be significant [1, 20]. For this reason, these remarkable findings have been attributed to fractionalized excitations analogous to those found in the spin liquid ground state of the Kitaev model [5, 6]. Recent discovery of quantization of the thermal Hall signal in the intermediate magnetic field phase has further stimulated interest in this material [8].

Understanding the salient features of magnetism in α -RuCl₃ requires a good knowledge of the magnetic interactions between the ruthenium magnetic moments. The magnetic Hamiltonian relevant to this material includes an isotropic Heisenberg (J) term as well as bond-dependent anisotropic Kitaev (K), and off-diagonal Γ terms [16]. The general Hamiltonian for atoms at adjacent sites i and j takes the following form, where $\alpha, \beta,$

and γ denote the spin components:

$$\mathcal{H}_{ij}^{(\gamma)} = JS_i \cdot S_j + KS_i^\gamma S_j^\gamma + \Gamma(S_i^\alpha S_j^\beta + S_i^\beta S_j^\alpha). \quad (1)$$

Often included in this Hamiltonian are further-neighbour isotropic interactions ($J_2, J_3,$ etc.) and additional off-diagonal term Γ' due to non-zero trigonal crystal fields [16, 17, 21]. Early *ab initio* calculations [9] and fits to inelastic neutron scattering measurements [5, 6] suggested an antiferromagnetic Kitaev interaction ($K > 0$). However, later calculations using the updated monoclinic crystal structure [4] instead suggested that the Kitaev term is ferromagnetic ($K < 0$) [10–15].

Although these scenarios can be distinguished by the direction of the ordered magnetic moment [22], to date, this information has not been experimentally available. The magnetic structural solution from neutron diffraction data [23] suggested two possible structures, with collinear moments confined to the monoclinic ac plane (See Fig. 1a). These two magnetic structures, differing only in the canting angle of the moment direction out of the crystallographic ab (honeycomb) plane (Θ), were fit equally well by the neutron data. In the case of $K > 0$, the moment is expected to point along the local cubic axis (towards a Cl atom), and therefore $\Theta = -35^\circ$, while $\Theta = +35^\circ$ corresponds to a ferromagnetic K ($K < 0$).

This ambiguity can be resolved with resonant elastic x-ray scattering (REXS). The magnetic scattering process in x-ray diffraction is fundamentally different from that of neutron diffraction, allowing the moment direction to be determined by measuring the *azimuthal* dependence of a magnetic Bragg peak intensity. This measurement is done by rotating the sample around the scattering vector (\vec{q}) as shown in Fig. 2a. With the incident linear polarization perpendicular to the vertical scattering plane, the diffracted magnetic intensity for electric dipole transitions is proportional to the projection of the ordered moment onto the scattered beam [24] and shows modulation as the sample is rotated about the scattering vector. By modelling this intensity modulation as a function of the azimuthal angle, Ψ , one can distinguish between the two possible structures suggested by the neutron measurement.

We have collected REXS data on a single crystal sample of α -RuCl₃ at the known magnetic Bragg peak position expected for zigzag magnetic ordering [2, 5]. The magnetic diffraction signal in this sample was first characterized by measuring its dependence on momentum,

arXiv:1910.13390v1 [cond-mat.str-el] 29 Oct 2019

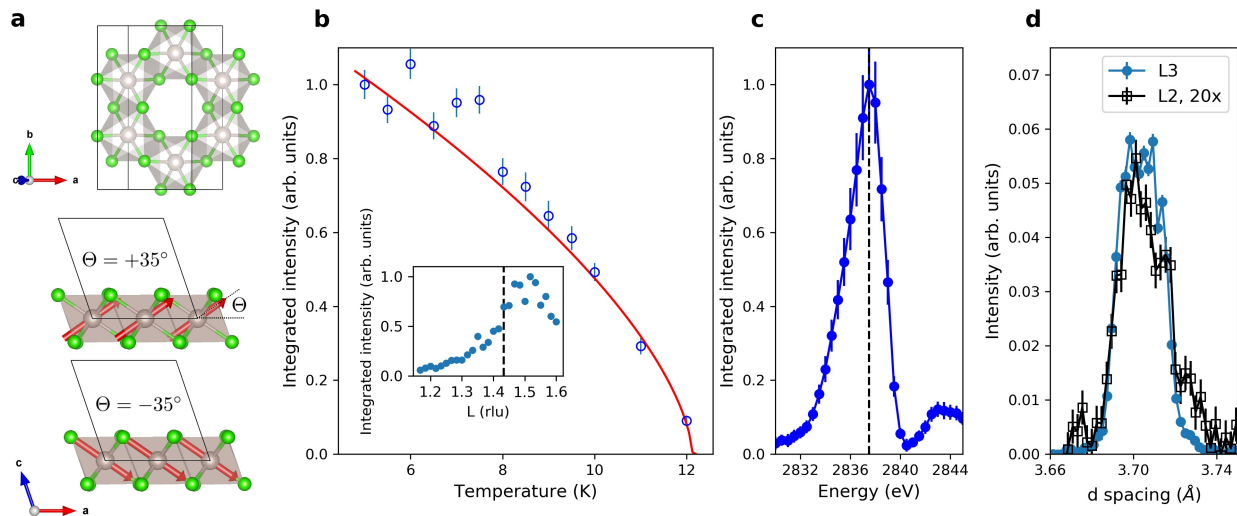


FIG. 1. **Characterization of magnetic scattering.** **a.** Crystal structure and ordered moment directions of α -RuCl₃ proposed in Ref. [23]. **b.** Temperature dependence of magnetic diffraction intensity at (0,-1,1.43), showing an ordering temperature of 12K. At each temperature the magnetic peak was measured by simultaneously scanning the sample and detector angles. Inset: intensity dependence on L reciprocal space direction (perpendicular to the honeycomb plane) showing a broad peak at the L=1.5 position. At each L value, the magnetic peak was measured by scanning along the momentum space K direction. The integrated intensities for all scans were found by fitting the scans with a Gaussian peak shape. Error bars shown are the square root of covariance value from the fit. **c.** Energy dependence of the magnetic diffraction intensity at (0,-1,1.43), showing resonance at the Ru L_3 resonant energy of 2837.5 eV. Integrated intensities and error bars were calculated from combined scans of the sample and detector angles, as in **b.** **d.** Comparison of the magnetic signals obtained with the incident photon energy at the Ru L_3 edge (2837.5 eV) and the Ru L_2 edge (2970 eV). Scans were collected by simultaneously scanning sample and detector angles. Error bars shown are the square root of the number of photons detected. A constant background was subtracted, and the overall photon counts normalized to the monitor recording incident beam intensity.

temperature, and incident photon energy. The momentum dependence of the magnetic signal showed an extended rod in the out-of-plane direction, with a broad peak at the position expected for ABAB type layer stacking as shown in Fig. 1b (inset). This stacking order has previously been reported in neutron diffraction measurements with an ordering temperature of 14 K, as opposed to the 7 K ordering temperature observed for the three-layer stacking [5]. We measured an ordering temperature of 12 K for this sample, as shown in Fig. 1b. We note that diffraction measurements at this x-ray energy will be highly surface-sensitive, since the beam penetrates the sample to a depth of only a few hundred nm, and the observed 2-layer stacking may not reflect the bulk crystal structure. As the magnetic interactions are strongly two-dimensional, we do not anticipate that stacking has a large effect on the moment direction. Scans along the L direction in reciprocal space were also collected at several different azimuthal positions, to ensure that the azimuthal dependence does not depend on the L position selected. The position L=1.43 was selected to maximize intensity while maintaining an accessible position for the diffractometer.

The azimuthal dependent measurement was collected at an incident photon energy of 2837.5 eV (corresponding to the Ru L_3 edge), where the intensity is at a maximum.

The dependence of the peak intensity on the incident photon energy was measured both to find the optimal energy for measurement, and to confirm the resonant nature of the magnetic peak. This energy dependence is plotted in Fig. 1c. Following the measurements at the L_3 edge, the magnetic peak intensity at the same reciprocal space position was also measured at the ruthenium L_2 edge (incident photon energy 2970 eV). The integrated intensity was substantially weaker at the L_2 edge (comparison is shown in Fig. 1d), and we calculate a ratio of approximately 20 for the intensities at the two photon energies.

The detailed azimuthal dependence of the magnetic scattering measured at the (0,-1,1.43) reciprocal lattice position is shown in Fig. 2b, which exhibits substantial variation in intensity as the sample is rotated about \vec{q} . The zero position of the azimuthal angle Ψ corresponds to the orientation with the in-plane direction (-2,0,0.65) pointing along the outgoing beam. The maxima in intensity correspond to the positions when the moment lies in the scattering plane, while the minima are at positions where the magnetic moment lies approximately orthogonal to the scattering plane. The difference in intensity of the two maxima is directly related to the degree of out-of-plane canting, with the largest peak directly indicating which way the moment is canted out of the honeycomb

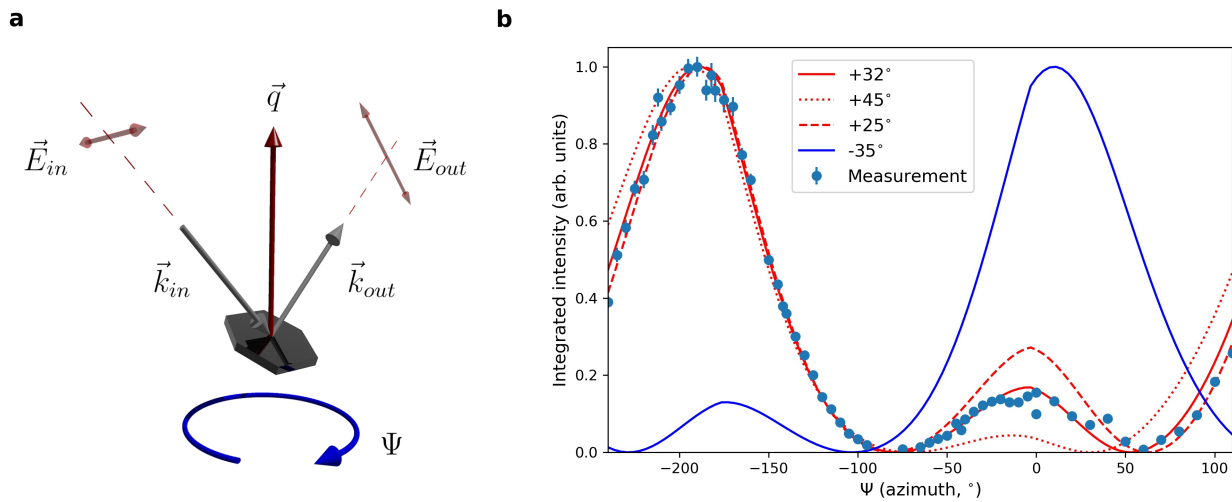


FIG. 2. **Azimuthal dependence.** **a.** Schematic diagram showing the geometry of the REXS experiment. **b.** Azimuthal dependence of the magnetic diffraction signal at $(0,-1,1.43)$. The azimuthal dependence is fit best with a magnetic moment angle of $\theta = +32^\circ$. The modeled intensities for $\Theta = +25^\circ$, $+45^\circ$ and -35° are shown for comparison. $\Psi = 0$ corresponds to the position with the in-plane direction $(-2,0,0.65)$ pointing along the scattered beam. The magnetic peak was measured by scanning the sample angle. Integrated intensities were found by fitting the scans with a Gaussian peak shape. Error bars shown are the square root of the covariance value from the fit.

plane. This can be seen in the modeled intensity for the two proposed moment directions (Fig. 2b), which show opposite behaviour in this respect. The measured azimuthal dependence collected for α - RuCl_3 is clearly fit best by the model with the moment direction pointing towards the RuCl_6 octahedral face, indicating that the moment direction is along the face-centered direction expected in the case of a ferromagnetic Kitaev term.

We also allow the angle within the ac plane (Θ) to vary as shown in dashed lines in Fig. 2b. The best fit is obtained when the moment is confined to the ac plane, with $\Theta = 32^\circ \pm 3^\circ$. This result is consistent with one of the two models proposed by the neutron diffraction result, and also provides insight into the form of the magnetic Hamiltonian. In the case of a ferromagnetic K term, Chaloupka and Khaliullin showed that a substantial antiferromagnetic Γ interaction term is required to keep the moment in the ac plane. Specifically they showed that with increasing Γ , the moment rotates away from the local octahedral xy plane ($\Theta \sim 50^\circ$) and slowly approaches $\Theta = 32^\circ$ from the positive side. According to Ref. [22], in order to have $\Theta \sim 32^\circ$ the magnitude of Γ must be a significant fraction of, or even exceed the magnitude of K . We note that $\Theta \sim 45^\circ$ was obtained for another Kitaev material Na_2IrO_3 [25], which would suggest that the Γ term is much smaller in Na_2IrO_3 .

Our REXS results provide a clue for solving one of the remaining questions regarding the magnetic properties of α - RuCl_3 : its large magnetic anisotropy. As reported by many groups [2, 4, 26, 27], the in-plane magnetic susceptibility measured by applying magnetic field along the di-

rection in the ab plane is significantly larger than the out-of-plane susceptibility. A conventional way to explain this would be resorting to the g -factor anisotropy. However, experimental data suggest that g -factor anisotropy cannot be very large, certainly not large enough to account for the anisotropic susceptibility [28, 29]. Another route to obtain a large magnetic anisotropy is via a large Γ term as suggested in Ref. [30]. Physically, the effect of the Γ interaction is to force the moments towards the ab plane, which accentuates magnetic anisotropy.

We demonstrate that a large Γ is sufficient to explain the observed magnetic anisotropy by comparing the experimental data with theoretical calculation results. The low-field magnetization data for fields applied in-plane and out-of-plane are plotted in Fig. 3, which shows that the susceptibility (slope) anisotropy is about $\chi_{ab}/\chi_c \sim 8$. This data is fit with the classical JKT model (Eq. (1)), where the model parameters are chosen to be consistent with the magnetic moment direction determined by REXS. Either a small Γ' or J_3 term was added to ensure the zigzag ground state of the model (details about the calculation are provided in the Supplementary Information). The data can be fitted for several parameter choices with ferromagnetic K and antiferromagnetic Γ of similar magnitude, demonstrating that the magnetization data can be explained without resorting to g -factor anisotropy. We note that in [30] it was shown that a ratio of $|\Gamma/K| \sim 1$ can also explain the star-shaped continuum intensity centered around the Brillouin zone center observed in inelastic neutron scattering [6].

The measurements outlined in this paper have deter-

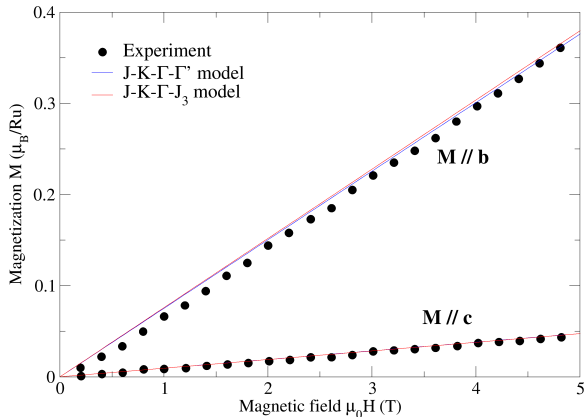


FIG. 3. Fitting the experimental data through simulated annealing calculations on the classical spin model. The experimental measurements were carried out using a commercial SQUID magnetometer at 2 K. The two representative parametrizations theory-I and theory-II correspond to $(J, K, \Gamma, \Gamma') = (-2.7, -10, 10.6, -0.9)$ and $(J, K, \Gamma, J_3) = (-1.5, -10, 8.8, 0.4)$, which yield the angles $\Theta = 33.3^\circ$ and $\Theta = 34.3^\circ$ between the moments and the honeycomb plane at zero field, respectively. Energy is in units of meV. The magnetization curves of these two parameterizations are very similar such that they overlap each other. We fix $g = 2.3$ and $S = 1/2$ throughout the calculations.

mined that the ordered moment direction in α - RuCl_3 points toward the octahedral face, rather than towards one of the cubic axes of the RuCl_6 octahedra. This result establishes that the Kitaev interaction is ferromagnetic in this material. In addition, we show that a substantial antiferromagnetic Γ interaction is essential for understanding magnetism of α - RuCl_3 . In particular, the presence of large Γ interaction could reconcile the large magnetic anisotropy observed experimentally with the almost isotropic g -factors expected in this material. The findings of our REXS measurement provide new experimental constraints on the magnetic Hamiltonian of α - RuCl_3 , indicating that it lies within the ferromagnetic K, antiferromagnetic Γ regime [22]. This result is in agreement with the findings of a number of ab-initio calculations, and can inform future investigations into the unusual magnetic behavior of α - RuCl_3 .

METHODS

REXS measurements were carried out at the beamline P09 at PETRA III at DESY (see [31] for details) at the ruthenium L_3 and L_2 edges (2838 and 2967 keV respectively). Most of the measurements, including mo-

mentum, temperature, and azimuthal dependence were collected at the L_3 edge. The magnetic intensity was also measured at the L_2 edge to determine the branching ratio. The monochromator was detuned to minimize the presence of higher harmonics in the beam, and the measurements were made with a sodium iodide scintillation detector. An all-in-vacuum path was used to minimize x-ray absorption by air. α - RuCl_3 single crystals were grown by vacuum sublimation in sealed quartz tubes using commercial RuCl_3 powder. The single crystal used for this measurement was a flat plate with largest dimension $\sim 400 \mu\text{m}$.

The orientation of the crystal used for this measurement was checked at room temperature with the crystal in the known monoclinic structural phase, by checking structural Bragg peaks using higher energy (third harmonic) photons. The crystal was also checked to ensure that it did not possess a twin rotated by 180° , which would affect the result of the azimuthal measurement. This was done by searching for structural peaks at the positions expected for the rotated structure. No intensity was found at the peak positions expected for the rotated crystal structure. The azimuthal dependence data was corrected for beam absorption (as described in [32]), and the beam footprint on the sample. Beam footprint on the sample was calculated from the angle between the sample surface and the incoming beam, and depended only on the ratio of the beam height and the smallest dimension of the sample. This ratio of beam height to sample size, and the magnetic moment angle Θ were the only parameters refined in the fit of the azimuthal dependence data. More detailed information about the fitting procedure can be found in the Supplementary Information.

ACKNOWLEDGEMENTS

We would like to thank Joel Bertinshaw and Hakuto Suzuki for their help with the experiment. We acknowledge DESY (Hamburg, Germany), a member of the Helmholtz Association HGF, for the provision of experimental facilities. Parts of this research were carried out at PETRA III. Work at the University of Toronto was supported by the Natural Science and Engineering Research Council (NSERC) of Canada, Canadian Foundation for Innovation, Ontario Innovation Trust, and the Center for Quantum Materials at the University of Toronto. Y.B.K. is also supported by the Killam Research Fellowship from the Canada Council for the Arts. This work was performed in part at Aspen Center for Physics, which is supported by National Science Foundation grant PHY-1607611.

-
- [1] Plumb, K. W. et al. α -RuCl₃: A spin-orbit assisted Mott insulator on a honeycomb lattice. *Phys. Rev. B* **90**, 041112(R) (2014).
- [2] Sears, J. A. et al. Magnetic order in α -RuCl₃: a honeycomb-lattice quantum magnet with strong spin-orbit coupling. *Phys. Rev. B* **91**, 144420 (2015).
- [3] Sandilands, L. J., Tian, Y., Plumb, K. W., Kim, Y.-J., & Burch, K. S. Scattering continuum and possible fractionalized excitations in α -RuCl₃. *Phys. Rev. Lett.* **114**, 147201-147205 (2015).
- [4] Johnson, R. D. et al. Monoclinic crystal structure of α -RuCl₃ and the zigzag antiferromagnetic ground state. *Phys. Rev. B* **92**, 235119 (2015).
- [5] Banerjee, A. et al. Proximate Kitaev quantum spin liquid behaviour in a honeycomb magnet. *Nat. Mat.* **15**, 733-740 (2016).
- [6] Banerjee, A. et al. Neutron scattering in the proximate quantum spin liquid α -RuCl₃. *Science* **356**, 1055-1059 (2017).
- [7] Do, S.-H. et al. Majorana fermions in the Kitaev quantum spin system α -RuCl₃. *Nat. Phys.* **13**, 1079-1084 (2017).
- [8] Kasahara, Y. et al. Majorana quantization and half-integer thermal quantum Hall effect in a Kitaev spin liquid. *Nature* **559**, 228 (2018).
- [9] Kim, H.-S., Shankar, V. V., Catuneanu, A. & Kee, H.-Y. Kitaev magnetism in honeycomb RuCl₃ with intermediate spin-orbit coupling. *Phys. Rev. B* **91**, 241110(R) (2015).
- [10] Kim, H.-S. & Kee H.-Y. Crystal structure and magnetism in α -RuCl₃: an ab initio study. *Phys. Rev. B* **93**, 155143 (2016).
- [11] Winter, S. M., Li, Y., Jeschke, H. O. & Valentí, R. Challenges in design of Kitaev materials: magnetic interactions from competing energy scales. *Phys. Rev. B* **93**, 214431 (2016).
- [12] Yadav, R. et al. Kitaev exchange and field-induced quantum spin-liquid states in honeycomb α -RuCl₃. *Sci. Rep.* **6**, 37925 (2016).
- [13] Hou, Y. S., Xiang, H. J. & Gong, X. G. Unveiling magnetic interactions of ruthenium trichloride via constraining direction of orbital moments: potential routes to realize a quantum spin liquid. *Phys. Rev. B* **96**, 054410 (2017).
- [14] Wang, W., Dong, Z.-Y., Yu, S.-L. & Li, J.-X. Theoretical investigation of magnetic dynamics in α -RuCl₃. *Phys. Rev. B* **96**, 115103 (2017).
- [15] Eichstaedt, C. et al. Deriving models for the Kitaev spin-liquid candidate material α -RuCl₃ from first principles. Preprint at <https://arxiv.org/abs/1904.01523> (2019).
- [16] Rau, J. G., Lee, E. K.-H. & Kee, H.-Y. Generic spin model for the honeycomb iridates beyond the Kitaev limit. *Phys. Rev. Lett.* **112**, 077204 (2014).
- [17] Katukuri, V. M. et al. Kitaev interactions between $j = 1/2$ moments in honeycomb Na₂IrO₃ are large and ferromagnetic: insights from ab initio quantum chemistry calculations. *New J. Phys.* **16**, 013056 (2014).
- [18] Chaloupka, J. & Khaliullin, G. Hidden symmetries of the extended Kitaev-Heisenberg model: Implications for the honeycomb-lattice iridates A₂IrO₃. *Phys. Rev. B* **92**, 024413 (2015).
- [19] Kitaev, A. Anyons in an exactly solved model and beyond. *Ann. Phys.* **321**, 2-111 (2006).
- [20] Jackeli, G. & Khaliullin, G. Mott insulators in the strong spin-orbit coupling limit: from Heisenberg to a quantum compass and Kitaev models. *Phys. Rev. Lett.* **102**, 017205-017209 (2009).
- [21] Yamaji, Y., Nomura, Y., Kurita, M., Arita, R., & Imada, M. First-principles study of the honeycomb-lattice iridates Na₂IrO₃ in the presence of strong spin-orbit interaction and electron correlations. *Phys. Rev. Lett.* **113**, 107201 (2014).
- [22] Chaloupka, J. & Khaliullin, G. Magnetic anisotropy in the Kitaev model systems Na₂IrO₃ and RuCl₃. *Phys. Rev. B* **94**, 064435 (2016).
- [23] Cao, H. B. et al. Low-temperature crystal and magnetic structure of α -RuCl₃. *Phys. Rev. B* **93**, 134423 (2016).
- [24] Hill, J. P. & McMorro D. F. Resonant exchange scattering: polarization dependence and correlation functions. *Acta Crystallogr. A* **52**, 236-244 (1996).
- [25] Chun, S. H. et al. Direct evidence for dominant bond-directional interactions in a honeycomb lattice iridate Na₂IrO₃. *Nature Physics* **11**, 462466 (2015).
- [26] Kubota, Y. et al. Successive magnetic phase transitions in α -RuCl₃: XY-like frustrated magnet on the honeycomb lattice. *Phys. Rev. B* **91**, 094422 (2015).
- [27] Majumder, M. et al. Anisotropic Ru³⁺ 4d⁵ magnetism in the α -RuCl₃ honeycomb system: Susceptibility, specific heat, and zero-field NMR. *Phys. Rev. B* **91**, 180401(R) (2015).
- [28] Agrestini, S. et al. Electronically highly cubic conditions for Ru in α -RuCl₃. *Phys. Rev. B* **96**, 161107(R) (2017).
- [29] Lampen-Kelley, P. et al. Anisotropic susceptibilities in the honeycomb Kitaev system α -RuCl₃. *Phys. Rev. B* **98**, 100403(R) (2018).
- [30] Gohlke, M. et al. Quantum spin liquid signatures in Kitaev-like frustrated magnets. *Phys. Rev. B* **97**, 075126 (2018).
- [31] Stremper, J. et al. Resonant scattering and diffraction beamline P09 at PETRA III. *J. Synchrotron Rad.* **20**, 541-549 (2013).
- [32] Brückel, T. et al. Antiferromagnetic order and phase transitions in GdS as studied with X-ray resonance-exchange scattering. *Eur. Phys. J. B* **19**, 475-490 (2001).